Effects of Sr and Cr doping on properties of $La_2Mo_2O_9$ electrolytes

KWANG SOO YOO*
Department of Materials Science and Engineering, University of Seoul, 90 Jeonnong-dong, Dongaemun-gu, Seoul 130-743, Korea
E-mail: ksyoo@uos.ac.kr

ALLAN J. JACOBSON
Center for Materials Chemistry, Department of Chemistry, University of Houston, Houston, Texas 77204-5641, USA
E-mail: ajjacob@uh.edu

Ion conductors are the basis for many electronic ceramics used in chemical sensors and fuel cells [1]. A typical example is yttria stabilized zirconia (YSZ) with the fluorite structure which is used as the oxygen sensor to monitor combustion and to control the optimum air/fuel ratio in virtually all modern automobiles.

Another application of YSZ is in solid oxide fuel cells (SOFCs) which operate at temperatures of around 1273 K. SOFCs have several advantages over molten carbonate fuel cells and phosphoric acid fuel cells particularly in fuel flexibility. The high operating temperature, however, causes material problems including microstructure changes of each cell component, solid state reaction between the electrolyte and the electrodes, and with thermal cycling due to thermal expansion mismatches. Therefore, it is desirable to operate the SOFC at as low temperature as possible. The operating temperature can be lowered by fabricating thinner electrolyte layers of conventional electrolyte materials or by developing new electrolyte materials with higher ionic conductivity [2–4]. $LaGaO_3$-based oxides are examples of new oxide ion conductors with the ABO_3 perovskite structure that have been studied by several investigators [4–6]. Doping $LaGaO_3$ with both Sr and Mg leads to high ion conductivity and the material is a promising electrolyte for SOFCs operating at intermediate temperatures.

In addition to YSZ with the fluorite structure and $LaGaO_3$ with the perovskite structure, examples of other oxygen-ion conductors are $Gd_2Zr_2O_7$ and $Gd_2Ti_2O_7$ with the pyrochlore structure [7, 8] and $La_2Mo_2O_9$ [9]. The parent compound $La_2Mo_2O_9$ discovered by Lacorre *et al.* [9–11] shows fast oxide-ion conducting properties above a reversible phase transformation at 853 K. At this temperature $La_2Mo_2O_9$ transforms from a slightly distorted low-temperature α–form to a cubic high-temperature β-form accompanied by an increase of conductivity of almost two orders of magnitude. At 1073 K, the conductivity is about 6×10^{-2} Scm^{-1}, which is comparable to that of YSZ, the most widely used oxide electrolyte [9]. Recently, dielectric relaxation studies on submicron crystalline $La_2Mo_2O_9$ and the effects of Ca doping on the oxygen ion diffusion and phase transition in $La_2Mo_2O_9$ were reported [12, 13].

In the present study, the effects of aliovalent doping (Sr and Cr on the La and Mo sites, respectively) on the thermal expansion coefficients and electrical conductivities of $La_2Mo_2O_9$ were systematically investigated. The crystal structure and electrical conductivity of $La_2Mo_2O_9$ have been reported previously [9–11]. The thermal expansion coefficient has not been determined, in spite of its importance in practical applications. In this paper, the thermal expansion coefficients and electrical conductivities are reported for pure and doped $La_2Mo_2O_9$.

The oxide compositions used in this experiments were $La_{2-x}Sr_xMo_{2-y}Cr_yO_{9-\delta}$ with $x = 0$ and 0.05 and $y = 0$ and 0.1, respectively, and the samples were prepared by typical ceramic powder processing and conventional solid-state reaction. The raw materials used were: La_2O_3 (99.999%, Cerac), SrO (99.9%, Aldrich), MoO_3 (99.999%, Cerac), and Cr_2O_3 (99.999%, Cerac). La_2O_3 was dried at 1273 K for 3 hr to remove CO_2 and adsorbed water. Powders of each sample were weighed to give the required composition, mechanically mixed and milled using a ball mill for 24 hr, and then uniaxially pressed into 25.4 mm diameter pellets. The pellets were calcined at 1273 K for 4 hr. The calcined samples were ground using an agate mortar and then pressed into 10 mm diameter pellets and rectangular bars with dimensions 3 mm × 3 mm × 7 mm. These samples were then sintered at 1523 K for 4 hr in air. The densities of the sintered samples measured by the Archimedes method were approximately 92% of theoretical value (5.62 g/cm^3 [14]).

The $La_{2-x}Sr_xMo_{2-y}Cr_yO_{9-\delta}$ samples were analyzed by powder X-ray diffraction using Cu K_α (1.5414 A) radiation (Rigaku). The powder samples were prepared by grinding to less than 10 μm in particle size. The thermal expansion behavior of the samples was measured in air from room temperature to 1173 K by using a dilatometer (Netzsch, DIL 402C). The bar specimens were heated and cooled at 2 K/min with a 2-hr hold at the maximum temperature. The thermal expansion coefficient was calculated from

*Author to whom all correspondence should be addressed.

0022–2461

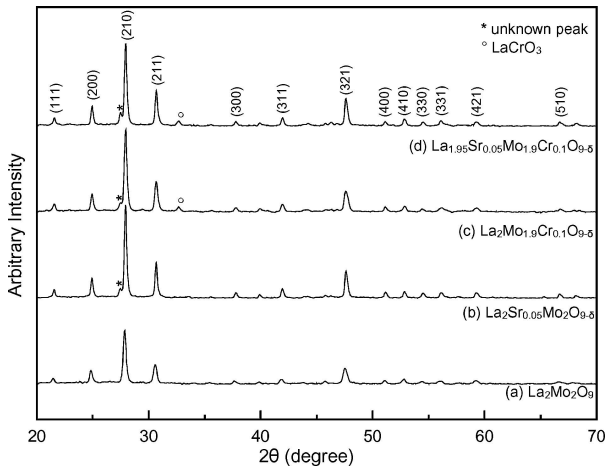

Figure 1 X-ray diffraction patterns of $La_{2-x}Sr_xMo_{2-y}Cr_yO_{9-\delta}$.

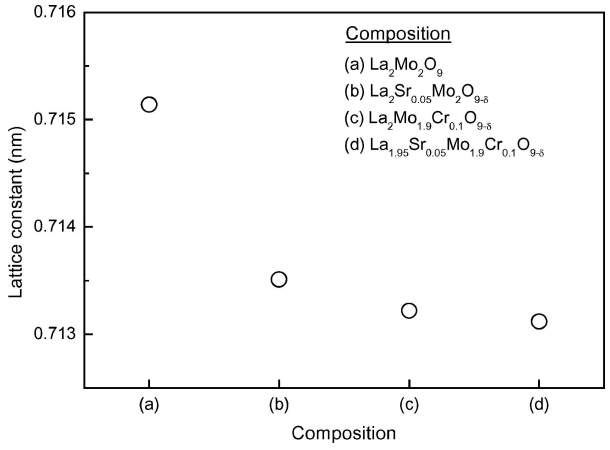

Figure 2 The variation of lattice constant of $La_{2-x}Sr_xMo_{2-y}Cr_yO_{9-\delta}$.

313 to 1173 K and the phase transition temperature was determined from the differential thermal expansion data. The electrical conductivity was determined by a computer-interfaced impedance analyzer (Hewlett Packard, 4192A) in the frequency range from 5 Hz to 13 MHz. The collected data were analyzed using EQUIVCRT modeling software. Further details can be found elsewhere [15].

Fig. 1 shows the X-ray diffraction (XRD) patterns of $La_{2-x}Sr_xMo_{2-y}Cr_yO_{9-\delta}$. As shown in Fig. 1a, pure $La_2Mo_2O_9$ without doping is cubic and this XRD pattern is in good agreement with JCPDS 28-0509 [16]. According to Lacorre *et al.* [9], the high-temperature form of the $La_2Mo_2O_9$ structure is cubic and cation arrangement is similar to that of the monazite structural type ($LnPO_4$). A plot for the lattice constant of $La_{2-x}Sr_xMo_{2-y}Cr_yO_{9-\delta}$ is shown in Fig. 2. Since Sr^{2+} and Cr^{3+} are smaller in size than La^{3+} and Mo^{6+}, respectively, and substitution of lower valent ions in the La^{3+} and Mo^{6+} sites leads to creation of oxygen vacancies, the cell volume decreases with Sr and Cr doping. A weak unknown peak at $2\theta = 27.4^\circ$ was found in the XRD patterns of the Sr- and Cr-doped samples and a trace of $LaCrO_3$ ($2\theta = 32.6^\circ$) was observed in the Cr-doped sample [16].

The percent linear thermal expansion versus temperature of $La_2Mo_2O_9$ is plotted in Fig. 3. As the result

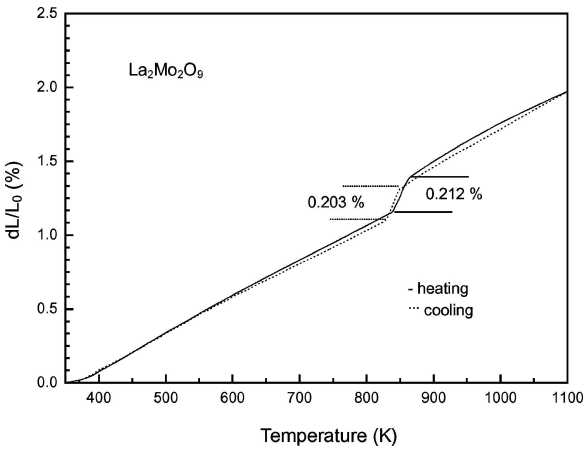

Figure 3 Percent linear thermal expansion versus temperature for $La_2Mo_2O_9$.

of determination from the differential thermal expansion data, the phase transition temperature on heating was 853 K. This temperature is in good agreement with the result previously reported [9]. A small hysteresis in the transition temperature on heating and cooling is observed and was also observed by Lacorre *et al.* [9] in differential thermal analysis data. The data were analyzed by linear regression at low-temperature for α-$La_2Mo_2O_9$ and at high-temperature for β-$La_2Mo_2O_9$. The difference in volume was calculated at the phase transition temperature under the assumption of the same change in all three dimensions. The linear changes on heating and cooling were 0.212 and 0.203%, respectively, and the changes in volume on heating and cooling were 0.605 and 0.591%, respectively. The thermal expansion coefficients on cooling were 22.8×10^{-6} K^{-1} at 673 K (α-$La_2Mo_2O_9$) and 24.9×10^{-6} K^{-1} at 973 K (β-$La_2Mo_2O_9$).

The thermal expansion coefficients (TECs) of electrolyte and electrodes are very important because the SOFCs are operated at high temperature. The TECs of the $La_2Mo_2O_9$-based electrolytes are similar to that of the cathode candidate, $LaCoO_3$ ($22 \sim 24 \times 10^{-6}$ K^{-1}) [17], and are greater than that of the electrolyte, YSZ (10×10^{-6} K^{-1}) [3]. Fig. 4 shows the percent linear thermal expansion on cooling of Sr- and Cr-doped $La_2Mo_2O_9$ samples. Both the phase transition

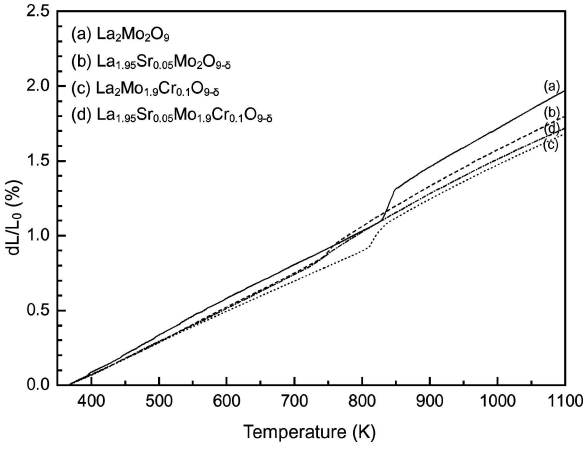

Figure 4 Percent linear thermal expansion versus temperature for $La_{2-x}Sr_xMo_{2-y}Cr_yO_{9-\delta}$.

TABLE I Thermal expansion coefficient (TEC), phase transition temperature, and volume change of $La_{2-x}Sr_xMo_{2-y}Cr_yO_{9-\delta}$

Samples	Phase transition temperature (K)	Volume change (%)	TEC ($\times 10^{-6}$ K^{-1}) 673 K	973 K
$La_2Mo_2O_9$	853	0.591	22.8	24.9
$La_{1.95}Sr_{0.05}Mo_2O_{9-\delta}$	783	0.189	24.1	25.4
$La_2Mo_{1.9}Cr_{0.1}O_{9-\delta}$	816	0.311	20.6	21.6
$La_{1.95}Sr_{0.05}Mo_{1.9}Cr_{0.1}O_{9-\delta}$	774	0.081	22.4	23.5

temperature and the linear change were affected by doping. In the case of $La_2Mo_{1.9}Cr_{0.1}O_{9-\delta}$, the phase transition temperature (816 K), the volume change, and the thermal expansion coefficients in both the low and high temperature regions are reduced. Addition of Sr alone in $La_{1.95}Sr_{0.05}MoO_{9-\delta}$ also leads to a lower transition temperature (783 K) and a lower volume change but to higher TEC values. Doping on both sublattices $La_{1.95}Sr_{0.05}Mo_{1.9}Cr_{0.1}O_{9-\delta}$gives the smallest volume change at the transition temperature (0.081%), a transition temperature of 774 K and TECs intermediate between those of the singly doped compositions. Thermal expansion coefficients, phase transition temperatures, and volume changes of $La_{2-x}Sr_xMo_{2-y}Cr_yO_{9-\delta}$ are listed in Table I. $La_2Mo_2O_9$ shows a phase transition at 853 K and exhibits high oxide-ion conductivity above the phase transition temperature [9]. Fig. 5 shows the Arrhenius plot for the electrical conductivity of $La_{2-x}Sr_xMo_{2-y}Cr_yO_{9-\delta}$ btained from the impedance measurements. Above the phase transition temperature

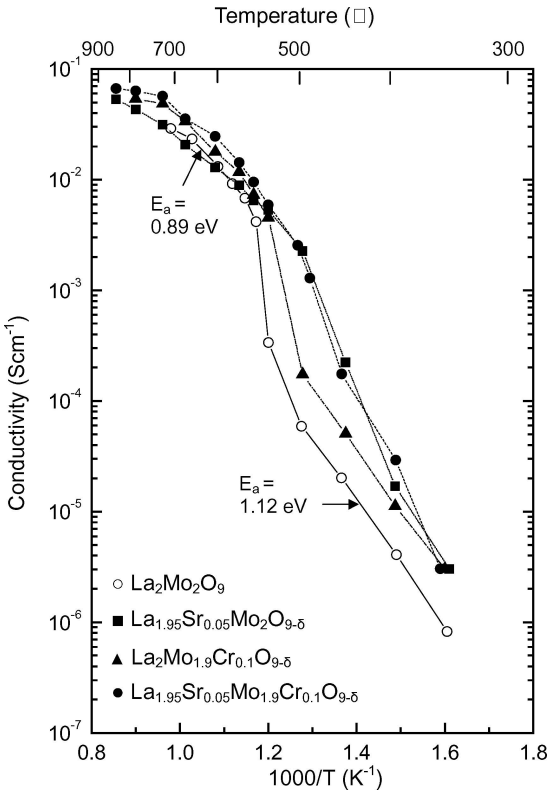

Figure 5 Arrhenius plots of electrical conductivity for $La_{2-x}Sr_xMo_{2-y}Cr_yO_{9-\delta}$. The lines serve as guide for the eye only.

(853 K) the conductivity is high (3×10^{-2} S cm^{-1} at 1023 K). As the temperature increases, the conductivity at the transition temperature increases abruptly by two orders of magnitude and the conductivity above and below the transition temperature increases linearly but with different slopes. The activation energies are approximately 0.89 and 1.12 eV for the high- and low-temperature phases, respectively. These results are closely similar to those reported by Lacorre *et al.* [9].

The temperature dependence of the electrical conductivity reflects the effect of dopants on the phase transition temperature as observed in the thermal expansion coefficient measurements. Below the phase transition temperature, the electrical conductivities of the electrolytes increased on doping with Sr and Cr. It is assumed that the increase of the conductivity is due to the introduction of the oxygen vacancies by the aliovalent doping. In particular, the electrical conductivities of $La_{1.95}Sr_{0.05}Mo_2O_{9-\delta}$ and $La_{1.95}Sr_{0.05}Mo_{1.9}Cr_{0.1}O_{9-\delta}$ near the transition temperature showed a smooth increase with increasing temperature without the abrupt change observed in pure $La_2Mo_2O_9$ and $La_2Mo_{1.9}Cr_{0.1}O_{9-\delta}$. The results are consistent with the changes in the volumes observed near the phase transition by dilatometry.

The ionic conductors, $La_{2-x}Sr_xMo_{2-y}Cr_yO_{9-\delta}$ ($x = 0, 0.05$ and $y = 0, 0.1$) were synthesized by solid-state reaction and their thermal expansion coefficients and electrical conductivities were characterized. The aliovalent dopants in $La_2Mo_2O_9$ affected the thermal expansion behavior, the phase transition temperature, and the electrical conductivity versus $1/T$ characteristics near the transition temperature. Specifically:

(1) The thermal expansion coefficients of $La_{2-x}Sr_xMo_{2-y}Cr_yO_{9-\delta}$ were approximately 20.6–25.4 $\times 10^{-6}$ K^{-1} and the introduction of dopants decreases the phase transition temperature and the volume change at the transition temperature.

(2) The electrical conductivities of Sr- and Cr-doped $La_2Mo_2O_9$ electrolytes above the transition temperature were slightly higher than that of pure $La_2Mo_2O_9$. In case of the Sr-doped compositions, the electrical conductivities near the transition temperature do not show the abrupt increase observed in pure $La_2Mo_2O_9$.

Acknowledgments

This work was partially supported by the R. A. Welch Foundation and their support is gratefully acknowledged. We would like to thank Mr. S. H. Park for assistance with the X-ray diffraction and thermal analysis.

References

1. Y.-M. CHIANG, D. BIRNIE and W. D. KINGERY, in "Physical Ceramics" (Wiley, New York, 1997) p. 185.
2. P. K. SRIVASTAVA, T. QUACH, Y. Y. DUAN, R. DONELSON, S. P. JIANG, F. T. CIACCHI and S. P. S. BADWAL, *Solid State Ionics* **99** (1997) 311.
3. B. C. H. STEELE, P. H. MIDDLETON and R. A. RUDKIN, *Solid State Ionics* **40–41** (1990) 388.
4. T. ISHIHARA, M. HONDA, T. SHIBAYAMA, H. MINAMI, H. NISHIGUCHI and Y. TAKITA, *J. Electrochem. Soc.* **145** (1998) 3177.

5. P.-N. HUANG and A. PETRIC, *J. Electrochem. Soc.* **143** (1996) 1644.
6. K. HUANG, M. FENG and J. B. GOODENOUGH, *J. Amer. Ceram. Soc.* **79** (1996) 1100.
7. H. L. TULLER, *Solid State Ionics* **94** (1997) 63.
8. S. A. KRAMER and H. L. TULLER, *ibid.* **82** (1995) 15.
9. P. LACORRE, F. GOUTENOIRE, O. BOHNKE, R. RETOUX and Y. LALIGANT, *Nature* **404** (2000) 856.
10. F. GOUTENOIRE, O. ISNARD, R. RETOUX and P. LACORRE, *Chem. Mater.* **12** (2000) 2575.
11. P. LACORRE, *Solid State Sci.* **2** (2000) 755.
12. Z. G. YI, Q. F. FANG, X. P. WANG and G. G. ZHANG, *Solid State Ionics* **8920** (2003) 1.
13. X. P. WANG and Q. F. FANG, *ibid* **146** (2002) 185.
14. F. P. ALEKSEEV, E. I. GET'MAN, G. G. KOSHCHEEV and M. V. MOKHOSOEV, *Russ. J. Inorg. Chem.* **14** (1969) 1558.
15. K. S. YOO, D. Y. BYUN and A. J. JACOBSON, *J. Korean Ceram. Soc.* **38** (2001) 693.
16. JCPDS-ICDD, #28-0509 ($La_2Mo_2O_9$), #24-1016 ($LaCrO_3$) version 1.10 (1995).
17. N. Q. MINH and T. TAKAHASHI, in "Science and Technology of Ceramic Fuel Cells" (Elsevier, New York, 1995) p. 139.

Received 9 October 2004
and accepted 18 January 2005